PHYSICAL REVIEW A VOLUME 25, NUMBER 3 MARCH 1982

# Total-cross-section measurements for positrons and electrons colliding with $H_2$, $N_2$, and $CO_2$

K. R. Hoffman,* M. S. Dababneh,† Y. -F. Hsieh, W. E. Kauppila, V. Pol,‡ J. H. Smart,§ and T. S. Stein
*Department of Physics and Astronomy, Wayne State University, Detroit, Michigan 48202*
(Received 23 October 1981)

Total scattering cross sections have been measured in the same apparatus for positrons and electrons colliding with $H_2$, $N_2$, and $CO_2$ using a beam transmission technique. The projectile impact energies range from 1—500 eV for $e^+$-$H_2$, 2—500 eV for $e^-$-$H_2$, 0.5—750 eV for $e^+$-$N_2$, 2.2—700 eV for $e^-$-$N_2$, 0.5—60 eV for $e^+$-$CO_2$, and 2—50 eV for $e^-$-$CO_2$. The onset of positronium formation is clearly seen by an abrupt rise in the total cross sections for positrons colliding with each of the molecules at the respective positronium-formation thresholds. The positron measurements are compared with the electron measurements at intermediate energies for $H_2$ and $N_2$. This comparison reveals a merging of the cross sections for $H_2$ at energies above 200 eV, while for $N_2$ the electron results remain higher than the positron results at all energies. Estimates are made of potential experimental errors, as well as the experimental resolution for discrimination against projectiles scattered at small forward angles.

## I. INTRODUCTION

It is well known that electron-molecule collision processes play an important role in numerous areas, such as gaseous lasers and planetary atmospheres. Positrons, on the other hand, are very short lived when produced in our world of ordinary matter because of their natural tendency to annihilate with electrons. During the past decade 0.511-MeV positron annihilation gamma rays have been discovered coming from solar flares[1] and the direction toward the center of our galaxy.[2] The astrophysical interpretation[3,4] of the annihilation gamma rays, which can provide information on the type of environment that exists where they originate, requires information about the nature of positron interactions with atoms and molecules of astrophysical importance, primarily hydrogen. Experimental investigations of positron and electron scattering by molecules not only provide some direct information leading to a better understanding of the above-mentioned processes, but can also lead to a better understanding of approximations used in various scattering theories. Positrons differ from electrons only by the sign of their electric charge. As a result, electron and positron interactions with gases have interesting similarities and differences. One significant difference is that the projectile electron is indistinguishable from the atomic electrons, which gives rise to an exchange interaction that is not present in positron-molecule scattering. Since the positron and electron are oppositely charged, the static Coulomb interaction between the projectile and the undistorted molecule is repulsive for positrons and attractive for electrons. The polarization interaction is attractive for both particles. Since the static and polarization interactions add for electron scattering, and tend to cancel each other for positron scattering, the electron scattering cross sections will generally be larger than for positrons. At sufficiently high energies, the polarization and exchange interactions will become unimportant leaving only the static interaction with the result that the positron and electron scattering cross sections will merge with their values being given by the first Born approximation. Two phenomena that can occur only for positron scattering are free annihilation [appreciable only for energies much less than 1 eV (Ref. 5)] and positronium formation.

Direct experimental investigations of low-energy electron-molecule scattering processes have been made since the 1920's and were the subject of a relatively recent review article by Golden *et al.*[6] Lane[7] has more recently reviewed the theory of electron-molecule collisions. Some of the more interesting features observed in many electron-molecule scattering experiments are resonances, temporary negative-ion states, which have been extensively discussed in a review by Schulz.[8] In the

case of positron-molecule scattering experiments, Griffith and Heyland[9] have reviewed the total-cross-section measurements.

The main impetus of the present work is to measure total cross sections for positrons scattered by some common molecules and to compare these measurements with the corresponding electron total-cross-section measurements made in the same apparatus using the same procedure. It is of interest to search for the possible existence of broad shape resonances in positron scattering because they are readily observed in total electron scattering experiments. The electron measurements are also meaningful in that they can be compared directly with prior electron measurements and theoretical calculations, and these comparisons can provide information on the reliability of the present experiment. A preliminary report of the present measurements for low-energy positrons scattering from $H_2$, $N_2$, and $CO_2$ was made by Kauppila *et al.*[10]

## II. EXPERIMENTAL APPROACH AND ERROR ANALYSIS

The experimental apparatus and procedure is the same as that used in previous total-cross-section measurements reported from this laboratory,[11–15] except for the recent addition of a quadrupole mass spectrometer. Only a brief discussion of the experimental approach will be presented here. A Van de Graaff accelerator is used to generate an $^{11}C$ positron source from which a well-defined energy ($<0.1$-eV energy width) positron beam is produced.[16] The positron beam is then transmitted through a gas scattering region and detected by a channeltron electron multiplier. For the electron measurements a thermionic cathode (Philips type B) is substituted for the positron source. Total scattering cross sections $Q_T$ are deduced from the attenuation of the projectile beam by means of the expression

$$I = I_0 e^{-nLQ_T} , \tag{1}$$

where $I_0$ is the detected beam current without gas present in the scattering region, $I$ is the detected beam current with gas of number density $n$ present in the scattering region, and $L$ is the beam path length in the scattering region.

In using Eq. (1) it must be realized that any errors in the determination of the measurable quantities will result in errors in measured total cross sections. Using the same procedure to estimate experimental errors as used by Kauppila *et al.*[15] we obtain the error estimates listed in Table I. The reported "experimental error" estimates are obtained by taking the square root of the sum of the squares of each individual error component contributing to the potential errors in $I$, $I_0$, $n$, and $L$, as well as the statistical error. The "maximum errors" result from the direct addition of each individual component. Separate total errors are given for the absolute total-cross-section measurements and the positron and electron comparison cross section measurements by the same target gas because several of the individual error components would affect both the positron and electron measurements equally. As a result, the estimated errors for the comparison measurements are smaller. In the present total-cross-section measurements the total estimated errors are somewhat larger than those reported by Kauppila *et al.*[15] due to an added potential source of error that relates to a minor vacuum pumping-speed problem that developed during the course of the present intermediate-energy measurements. A standard check made in every data run is to measure cross sections for several different target gas densities to ensure that the results are independent of $n$. The measured cross sections for nine typical data runs for different projectile-gas combinations are shown in Fig. 1. In the present measurements the purity of each target gas was verified by the use of a quadrupole mass spectrometer.

TABLE I. Estimated percentage errors in the present absolute and $e^{\pm}$ comparison total-cross-section measurements. The "experimental errors" are shown outside the parentheses while the "maximum errors" are enclosed by the parentheses. The statistical errors in this table are typical values with the actual values for each data point listed in the Appendix. The estimated errors in this table do not include the potential errors associated with discrimination against small-angle scattering which are discussed separately.

| | Projectile | |
|---|---|---|
| | $e^+$ | $e^-$ |
| statistical | 2(2) | 1(1) |
| $I, I_0$ | 3(6) | 3(4.5) |
| $n$ | 4(8) | 4(8) |
| $L$ | 1(1.5) | 1(1) |
| Total (absolute) | 6(17.5) | 5(14.5) |
| Total ($e^{\pm}$ comparison) | 4(9) | 3(6) |

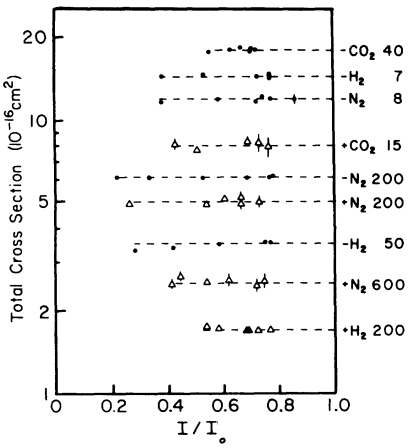


FIG. 1. Measured total cross sections versus attenuation ratio $I/I_0$ for various projectile-target combinations. The projectiles are labeled (+) for positrons and (−) for electrons. The numbers following the target gas symbols are the projectile energies in eV. Statistical uncertainties of one standard deviation are represented by the bars except where they are encompassed by the dots or triangles.

Another source of error, not included in Table I, relates to the inability of most transmission experiments to discriminate against all the projectile particles that are scattered at small angles in the forward direction. This lack of discrimination will result in the measurement of total cross sections that are too low. A detailed analysis of the present experimental system for this potential error has been made by Kauppila *et al.*,[15] who determined that two independent aspects of the experiment contribute to provide discrimination against small-angle scattering. These two aspects are (a) the use of a retarding potential field after the scattering region to serve as a potential "hill" that must be surmounted by the transmitted beam, and (b) the use of a small beam exit aperture from the scattering region. Using Eqs. (6) and (10) from Ref. 15 we obtain the estimated discrimination angles for the present measurements listed in Table II. Since the estimated discrimination angles for the retarding potential procedure and the exit aperture size are independent of each other it would be expected that the smaller angle for each particular projectile, energy, and target combination should represent an upper limit estimate of the actual angular discrimination. In general, the estimated angular discriminations listed in Table II for the electron measurements are smaller than for the positron measurements because it is much easier to optimize the beam-controlling parameters (lens elements and magnetic fields) for the more intense (typically 10 times larger) electron beam currents that are used. In order to determine the amount by which the measured total cross sections are too low, detailed information is required on the differential elastic scattering cross sections and, depending on the projectile energies, inelastic scattering cross sections. It should be mentioned that the present experiment discriminates almost completely against any inelas-

TABLE II. Estimated discrimination angles (in degrees) deduced for the retarding potential procedure ($R$ values) and for the effect due to the exit aperture size ($A$ values). The columns are also labeled according to the target gases and projectile particles.

| | $H_2$ | | $N_2$ | | $CO_2$ | |
|---|---|---|---|---|---|---|
| | $e^+$ | $e^-$ | $e^+$ | $e^-$ | $e^+$ | $e^-$ |
| $E$ (eV) | $R,A$ | $R,A$ | $R,A$ | $R,A$ | $R,A$ | $R,A$ |
| 5 | 25,38 | 14,6 | 19,32 | 19,6 | 22,36 | 11,5 |
| 10 | 20,22 | 18,11 | 15,29 | 10,6 | 19,33 | |
| 20 | 17,23 | 7,5 | 16,28 | 8,5 | 18,23 | 7,5 |
| 30 | | 7,5 | 22,22 | 7,5 | 14,22 | 5,5 |
| 50 | 19,21 | 7,5 | 17,21 | 6,5 | | |
| 75 | 24,17 | 6,5 | 19,13 | 11,5 | | |
| 100 | 20,18 | 7,5 | 18,13 | 5,5 | | |
| 200 | 30,11 | 5,5 | 16,8 | 8,5 | | |
| 300 | 28,9 | 7,5 | 21,8 | 8,5 | | |
| 400 | 16,14 | 8,5 | 25,8 | 8,5 | | |
| 500 | 11,15 | 7,5 | 12,8 | 7,5 | | |
| 600 | | | 16,8 | 7,5 | | |
| 700 | | | 22,9 | 6,5 | | |

tic scattering if the energy lost by the scattered projectile particles is more than a few tenths of an eV at low energies and a few eV at the higher energies due to the effect of the retarding element following the scattering region. In scattering from molecules, rotational and vibrational processes may contribute to this potential problem while electronic excitation, ionization, and positronium formation would not be problems. In the course of these total cross section measurements, we have noticed that small-angle scattering does affect our results because if we tune up the projectile beam with higher axial magnetic fields in our scattering region we obtain lower cross section values, which is consistent with an estimated poorer angular discrimination for these higher magnetic fields. It is for this reason that we attempt to tune up our projectile beams for the lowest feasible magnetic fields in the scattering region in order to obtain the best possible angular discriminations.

## III. RESULTS

In the following discussions concerning the present total-cross-section measurements it is necessary to realize that the estimated angular discriminations, given in Table I, could affect both the reported absolute total-cross-section values and the comparisons between the positron and electron measurements on the same target gas. The present total-cross-section measurements and associated statistical uncertainties are listed in the Appendix.

### A. $e^{\pm}$-$H_2$

The present results for low- and intermediate-energy positrons scattered by hydrogen molecules are presented in Figs. 2 and 3, respectively, along with some prior experimental results[17,18] and theoretical calculations.[19,20] Our measurements are in reasonable agreement with Coleman *et al.*[17] at energies less than 9 eV and are higher for energies above 9 eV. The present results average about 10% lower than the data of Charlton *et al.*[18] below 100 eV but are in good agreement with them at energies above 100 eV. Some earlier low- to intermediate-energy measurements (not shown in Figs. 2 and 3) by Coleman *et al.*,[21] which have been superseded by the more recent Coleman *et al.*[17] measurements, were recognized as being abnormally low at the higher energies due to the lack of discrimination against small-angle scattering. Both the

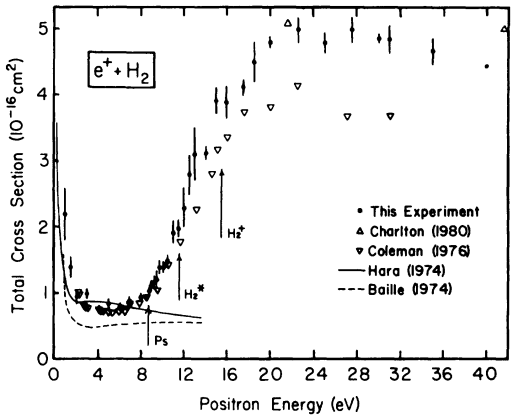


FIG. 2. Total positron-hydrogen molecule scattering cross-section results at low energies. The present results are shown with the experimental data of Coleman *et al.* (Ref. 17) and Charlton *et al.* (Ref. 18), and the theoretical calculations of Baille *et al.* (Ref. 19) and Hara (Ref. 20). Statistical uncertainties of the present results are represented by error bars when they are not encompassed by the size of the dot. The inelastic thresholds for positronium formation, electronic excitation, and ionization are indicated by arrows.

present measurements and those of Coleman *et al.*[17] show a sharp increase in the cross sections near the threshold for positronium formation and a gradual increase at the lowest energies. The large increase near the positronium-formation threshold may also be partly due to excitation of the repul-

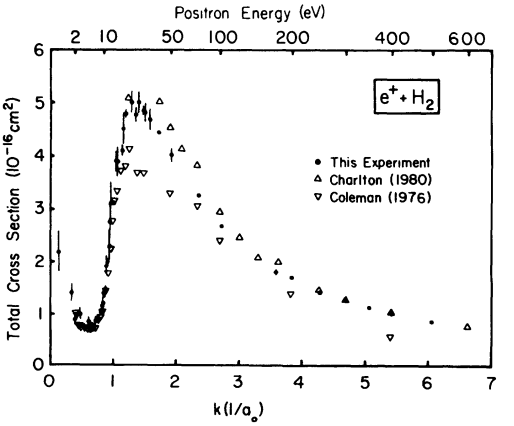


FIG. 3. Total positron-hydrogen molecule scattering cross-section results extending to intermediate energies. The present results are shown with the experimental data of Coleman *et al.* (Ref. 17) and Charlton *et al.* (Ref. 18). Other pertinent information is the same as for Fig. 2.

sive $^3\Sigma_u^+$ state, which becomes energetically possible in the vicinity of 9 eV. Relative measurements have recently been made by Charlton *et al.*[22] of the energy dependence of the orthopositronium-formation cross sections for molecular hydrogen which indicate a peak near the ionization threshold at 15.6 eV. This information may well indicate that other inelastic processes make appreciable contributions to the total cross section for energies above the ionization threshold since the total cross section continues to increase in this energy region. The calculation of the elastic scattering cross section by Hara,[20] using a fixed nuclei approximation, is in rather good agreement with the experiments mentioned above, as can be seen in Fig. 2, while the adiabatic-nuclei-approximation calculation of the elastic scattering cross section by Baille *et al.*[19] is somewhat lower in absolute values but similar in shape. By using the differential-cross-section results of Hara and the angular discriminations given in Table II it is estimated that the present measurements are less than 1% low at 10 eV and about 5% low at 5 eV.

The present measurements for electrons of low and intermediate energies colliding with hydrogen molecules are shown in Figs. 4 and 5, respectively, where they are compared with prior experimental results[23–28] and some theoretical calculations.[29–31] All of these results are in very good agreement in regard to the general shapes of the total-cross-section curves, reaching a maximum between 2 and 4 eV. Our results are in very good agreement (generally within 5%) with the recent measurements of van Wingerden *et al.*[27] and Dalba *et al.*[28] but are consistently higher (more than 10%) than the measurements of Golden *et al.*[25] and Bruche.[23] The measurements of Ramsauer and Kollath[24] and Ferch *et al.*[26] were taken at energies lower than the range of this experiment, but are included in Fig. 4 because they indicate an energy dependence similar to the other results shown. The theoretical results displayed in Fig. 4 are the elastic scattering cross sections of Wilkins and Taylor (a Hartree-Fock approach),[29] and of Hara (a two-center calculation including polarization),[30] and the total cross sections of Henry and Lane (a close-coupling calculation including polarization).[31] All of these theories account for exchange in some manner. The Henry and Lane results (which include rotational excitation as well as elastic scattering) for $H_2$ initially in the $j=0$ and $j=1$ rotational levels bracket our measurements with their $j=1$ curve being in agreement at the cross section maximum but lower

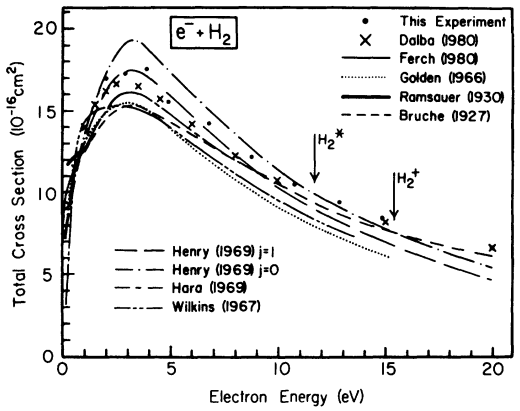


FIG. 4. Total electron-hydrogen molecule scattering cross-section results at low energies. The present results are shown with the experimental data of Bruche (Ref. 23), Ramsauer and Kollath (Ref. 24), Golden *et al.* (Ref. 25), Ferch *et al.* (Ref. 26), and Dalba *et al.* (Ref. 28), and the theoretical calculations of Wilkins and Taylor (Ref. 29), Hara (Ref. 30), and Henry and Lane (Ref. 31). Curves were used to represent the data points of Refs. 23–26 to enhance clarity. Other pertinent information is the same as for Fig. 2.

everywhere else, and the $j=0$ curve being in agreement in the vicinity of 12 eV and being higher at lower energies. An estimate of the potential error in the present total-cross-section measurements at 4.4 eV due to lack of discrimination against small-angle scattering has been made using the $j=0$ differential-cross-section results of Henry and

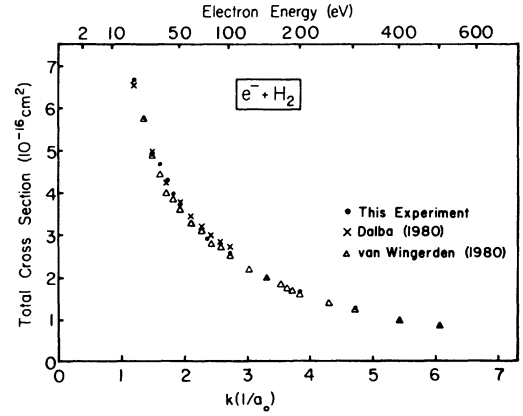


FIG. 5. Total electron-hydrogen molecule scattering cross-section results extending to intermediate energies. The present results are shown with the experimental data of van Wingerden *et al.* (Ref. 27) and Dalba *et al.* (Ref. 28). Other pertinent information is the same as for Fig. 2.

Lane, and it is found that this error would be less than 1%. At lower energies the theory of Henry and Lane indicates less forward scattering so this can be taken as a reasonable indication that our low energy $e^-$-$H_2$ results are not appreciably affected by the neglect of small-angle scattering.

A comparison of our positron and electron measurements in Fig. 6 illustrates how the electron total cross sections are much larger (more than 20 times) than the positron cross sections at low energies. This undoubtedly results from the tendency toward cancellation of the static and polarization potentials for positrons, while they add for electrons. The peak in the cross section curve for electrons (at about 3 eV) is associated primarily with elastic scattering, while the peak for positrons (in the vicinity of 25 eV) is most likely associated with inelastic processes. In the energy range from 30—200 eV the electron results are lower than the positron results, a somewhat anomalous behavior, most likely associated with the positron curve having a larger contribution from inelastic processes than for electrons. For energies above 200 eV the measured positron and electron total cross sections merge (to within 2%) and remain merged up to the highest energies (500 eV) investigated. It is not known what effect the experimental lack of complete angular discrimination against small-angle scattering has on the present measurements because the pertinent differential cross section information is not available at these intermediate energies.

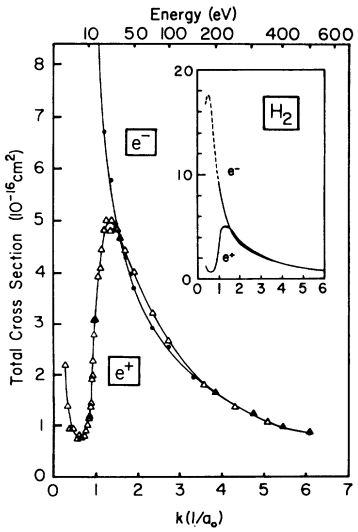


FIG. 6. A comparison of the total positron- and electron-hydrogen molecule scattering cross sections as measured by this experiment. The electron results are indicated by (●) and the positron results by (△ ).

### B. $e^{\pm}$-$N_2$

Our measurements for positrons colliding with molecular nitrogen are compared with prior experiments[18,21,32] and some theoretical calculations[33,34] in Figs. 7 and 8. The present results are in fair agreement with Charlton *et al.*,[18] although the shapes of the respective curves are somewhat different. Except for the energy region in the vicinity of 8 eV, the measurements of Coleman *et al.*[21] are appreciably lower than our results, particularly at the higher energies where their measurements are low due to neglect of small-angle scattering. The theoretical total (elastic plus rotational excitation) cross section curve of Gillespie and Thompson[34] is lower than the present results, while the elastic scattering cross section curve calculated by Darewych and Baille[33] (in the adiabatic approximation) crosses our results at 4 eV. The only differential elastic scattering data available, that are of interest to this experiment, are at 6.8 eV from Gillespie and Thompson which enables us to estimate that our measurements may be 20% too low. If the assumptions leading to this estimate are valid it would indicate an even larger discrepancy between our measurements and the prior experimental and theoretical results.

The present $e^-$-$N_2$ measurements are compared with prior experimental[23,35—38] and theoretical[39] results in Figs. 9 and 10. All of the displayed experimental data are in good agreement (generally within 10%). The $^2\Pi_g$ shape resonance in the vicinity of 2.4 eV was not investigated in our measurements due to the rather broad energy width of our electron beam [about 0.14 eV (Ref. 16)]. The "hybrid theory" calculation of Chandra and Temkin[39] gives total-cross-section results that exhibit the vibrational structure of the temporary $N_2^-$ ion state observed by Golden[35] and Kennerly.[36] Their theory is, however, about 15% higher than the experiments above and below the resonance region. Using the differential vibrationally elastic cross sections of Chandra and Temkin,[40] we estimate that our total-cross-section measurements would be less than 1% low at 5 eV and about 1% low at 10 eV.

A comparison of the present positron and electron total-cross-section measurements is made in Fig. 11 where it is seen that the electron total cross sections are larger than the positron values for all energies of comparison. At the highest energies of comparison (700 eV) there is no indication of a tendency toward merging of these cross section curves.

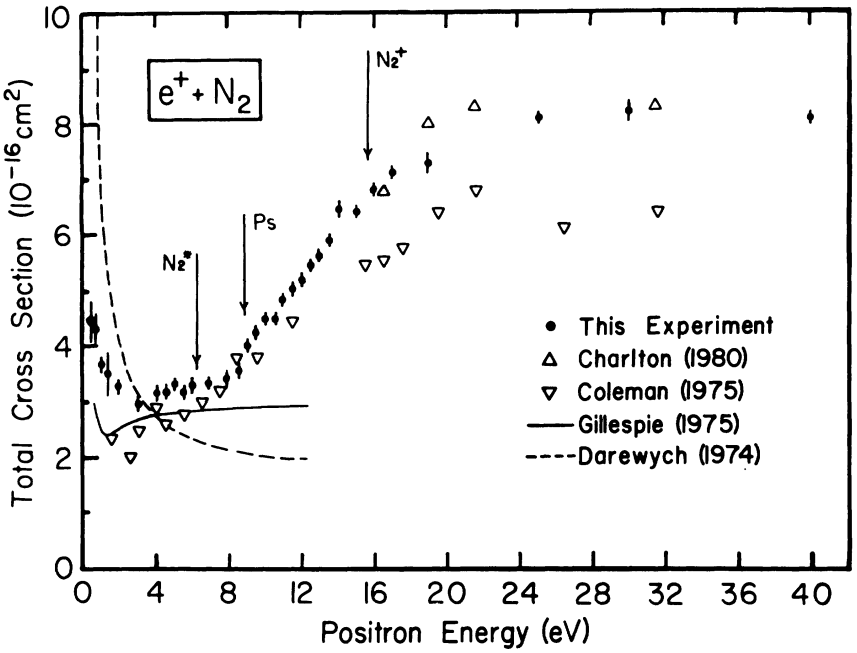


FIG. 7. Total positron-nitrogen molecule scattering cross-section results at low energies. The present results are shown with the experimental data of Coleman *et al.* (Refs. 21 and 32) and Charlton *et al.* (Ref. 18), and the theoretical calculations of Darewych and Baille (Ref. 33) and Gillespie and Thompson (Ref. 34). Other pertinent information is the same as for Fig. 2.

### C. $e^{\pm}$-$CO_2$

The present low-energy total-cross-section measurements for positron-$CO_2$ scattering are shown in Fig. 12, along with the measurements of Coleman *et al.*[32] and Charlton *et al.*[18] Our results differ markedly from those of Coleman *et al.* in that we are typically 50% higher, and our energy dependence reveals a distinct bump in the total-cross-section curve after the positronium-formation threshold at 7.0 eV and a rapidly increasing total cross section at the lowest energies. Our results are in better agreement (averaging less than 10% lower) with the recent measurements of Charlton *et al.*

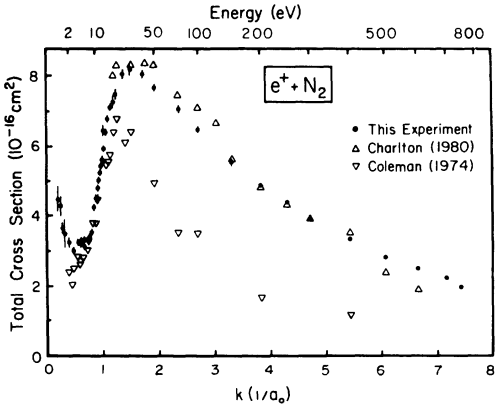


FIG. 8. Total positron-nitrogen molecule scattering cross-section results extending to intermediate energies. The present results are shown with the experimental data of Coleman *et al.* (Ref. 21) and Charlton *et al.* (Ref. 18). Other pertinent information is the same as for Fig. 2.

For low-energy electron-$CO_2$ scattering our results are compared with prior experimental[41–44] and theoretical[45] work in Fig. 13. The most striking feature of this total-cross-section curve is the broad shape resonance in the vicinity of 4 eV. It is interesting that our measurements agree very well (within 10%) with the measurements of Bruche,[41] Szmytkowski and Zubek,[43] and Ferch *et al.*[44] on both sides of the shape resonance, but are more than 15% higher at the peak. This observed behavior could be explained by the present experiment having a narrower beam energy width [about 0.14 eV (Ref. 16)], better discrimination against small-angle scattering (see Table II), or a combination of these two effects. Ferch *et al.* reported an energy resolution of 0.25 eV in the peak vicinity which could explain their results being lower than ours, while Szmytkowski and Zubek had an indi-

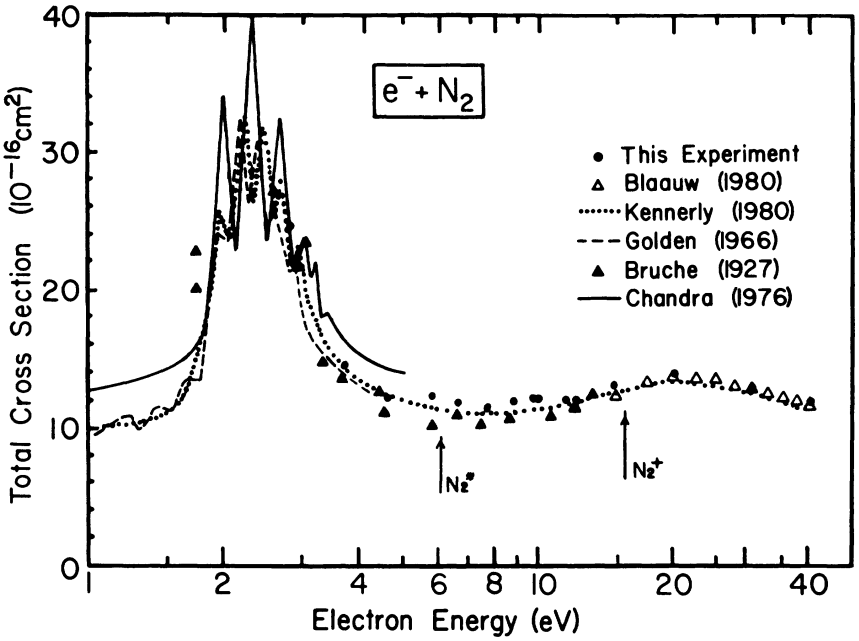


FIG. 9. Total electron-nitrogen molecule scattering cross-section results at low energies. The present results are shown with the experimental data of Bruche (Ref. 23), Golden (Ref. 35), Kennerly (Ref. 36), Blaauw *et al.* (Ref. 37), and Dalba *et al.* (Ref. 38), and the theoretical calculations of Chandra and Temkin (Ref. 39). Curves were used to represent the data points of Refs. 35 and 36 to enhance clarity. Other pertinent information is the same as for Fig. 2.

cated energy resolution of better than 0.05 eV which by itself should have resulted in a higher peak value for them. The "fixed nuclei" total-(elastic plus rotational excitation) cross-section calculation of Morrison *et al.*,[45] which agrees very well with the experiments for energies below the shape resonance, indicates appreciable forward (and backward) scattering at 4 eV. Using the results of this theory and our estimated angular discriminations given in Table II we estimate that our meas-

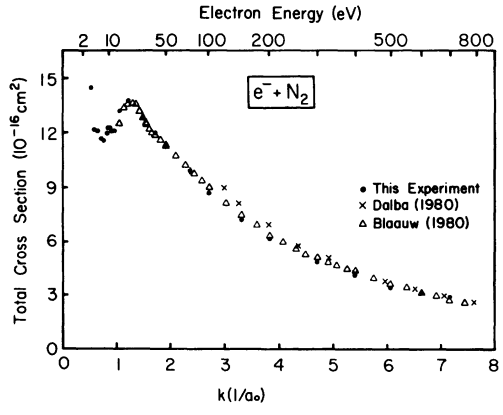


FIG. 10. Total electron-nitrogen molecule scattering cross-section results extending to intermediate energies. The present results are shown with the experimental data of Blaauw *et al.* (Ref. 37) and Dalba *et al.* (Ref. 38). Other pertinent information is the same as for Fig. 2.

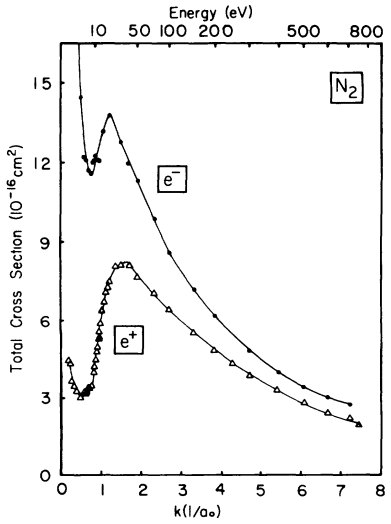


FIG. 11. A comparison of the total positron- and electron-nitrogen molecule scattering cross sections as measured by this experiment. The electron results are indicated by (●) and the positron results (△ ).

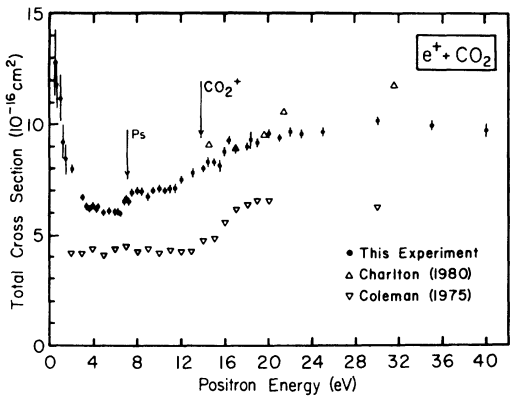


FIG. 12. Total positron—carbon-dioxide molecule scattering cross-section results at low energies. The present results are shown with the experimental data of Coleman *et al.* (Ref. 32) and Charlton *et al.* (Ref. 18). Other pertinent information is the same as for Fig. 2.

urements may be 1% too low at 4 eV and less than 1% too low at 10 eV. At higher energies the present results gradually become more than 10% larger than the measurements of Bruche.

It is of particular interest to compare the present $e^+$-$CO_2$ results (shown in Fig. 12) with the $e^-$-$CO_2$ results (shown in Fig. 13) because it is found

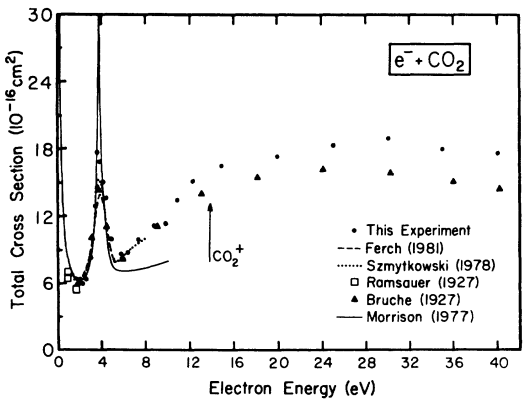


FIG. 13. Total electron—carbon-dioxide molecule scattering cross-section results at low energies. The present results are shown with the experimental data of Bruche (Ref. 41), Ramsauer (Ref. 42), Szmytkowski and Zubek (Ref. 43), and Ferch *et al.* (Ref. 44), and the theoretical calculation of Morrison *et al.* (Ref. 45). Only a representative sampling of the data points of Bruche are shown. Other pertinent information is the same as for Fig. 2.

that in the vicinity of (and possibly below) 2 eV the positron total cross sections are larger than the electron total cross sections. It is also found that, except for the electron shape resonance, the electron cross sections up to 40 eV are at most a factor of 2 larger than the corresponding positron values and the shapes of the respective curves are quite similar.

## ACKNOWLEDGMENTS

We gratefully acknowledge the helpful assistance of F. Laperriere, S. Smith, A. Sternad, W. Kaiser, and M. Scheuermann in various aspects of this project. This work was supported by the National Science Foundation under Grants Nos. PHY77-18760 and PHY80-07984.

## APPENDIX

Present total cross section results for various projectile-target combinations with statistical uncertainties:

$e^+$-$H_2$

| $E$(eV) | $Q(10^{-16}$ cm$^2)$ | $E$(eV) | $Q(10^{-16}$ cm$^2)$ |
|---|---|---|---|
| 1.0 | 2.2 ±0.4 | 15.0 | 3.9 ±0.2 |
| 1.5 | 1.40±0.15 | 16.0 | 3.9 ±0.25 |
| 2.0 | 0.94±0.12 | 17.5 | 4.12±0.12 |
| 3.0 | 0.95±0.09 | 18.5 | 4.5 ±0.3 |
| 4.0 | 0.77±0.07 | 20 | 4.82±0.08 |
| 5.0 | 0.84±0.08 | 22.5 | 5.0 ±0.2 |
| 6.0 | 0.79±0.07 | 25 | 4.8 ±0.15 |
| 7.0 | 0.88±0.08 | 27.5 | 5.0 ±0.2 |
| 8.0 | 0.91±0.07 | 30 | 4.87±0.08 |
| 8.5 | 0.91±0.08 | 31 | 4.85±0.2 |
| 8.75 | 1.03±0.08 | 35 | 4.7 ±0.2 |
| 9.0 | 1.10±0.10 | 40 | 4.44±0.05 |
| 9.25 | 1.17±0.10 | 50 | 4.01±0.10 |
| 9.5 | 1.21±0.12 | 75 | 3.25±0.02 |
| 9.75 | 1.40±0.11 | 100 | 2.68±0.02 |
| 10.0 | 1.40±0.10 | 175 | 1.83±0.05 |
| 10.5 | 1.48±0.10 | 200 | 1.71±0.02 |
| 11.0 | 1.92±0.20 | 250 | 1.37±0.03 |
| 11.5 | 1.98±0.12 | 300 | 1.27±0.02 |
| 12.0 | 2.3 ±0.3 | 350 | 1.13±0.02 |
| 12.5 | 2.8 ±0.3 | 400 | 1.00±0.02 |
| 13.0 | 3.1 ±0.4 | 500 | 0.86±0.01 |
| 14.0 | 3.12±0.10 | | |

(A1)

$e^+$-$N_2$

| $E$(eV) | $Q(10^{-16}$ cm$^2)$ | $E$(eV) | $Q(10^{-16}$ cm$^2)$ |
|---|---|---|---|
| 0.5 | 4.5 ±0.4 | 13.5 | 5.94±0.10 |
| 0.75 | 4.3 ±0.3 | 14 | 6.47±0.15 |
| 1.00 | 3.7 ±0.15 | 15 | 6.40±0.10 |
| 1.5 | 3.5 ±0.4 | 16 | 6.79±0.10 |
| 2.0 | 3.3 ±0.15 | 17 | 7.14±0.10 |
| 3.0 | 3.0 ±0.15 | 19 | 7.3 ±0.2 |
| 4.0 | 3.20±0.10 | 20 | 7.52±0.15 |
| 4.5 | 3.22±0.10 | 25 | 8.11±0.10 |
| 5.0 | 3.31±0.10 | 30 | 8.2 ±0.2 |
| 5.5 | 3.15±0.10 | 40 | 8.07±0.10 |
| 6.0 | 3.35±0.10 | 50 | 7.69±0.10 |
| 7.0 | 3.35±0.10 | 75 | 7.08±0.10 |
| 8.0 | 3.40±0.10 | 100 | 6.49±0.07 |
| 8.5 | 3.57±0.10 | 150 | 5.56±0.10 |
| 9.0 | 4.05±0.10 | 200 | 4.90±0.05 |
| 9.5 | 4.26±0.12 | 250 | 4.40±0.06 |
| 10.0 | 4.48±0.10 | 300 | 3.90±0.04 |
| 10.5 | 4.50±0.10 | 400 | 3.37±0.02 |
| 11.0 | 4.82±0.10 | 500 | 2.84±0.05 |
| 11.5 | 5.03±0.10 | 600 | 2.51±0.03 |
| 12.0 | 5.25±0.10 | 700 | 2.27±0.06 |
| 12.5 | 5.44±0.10 | 750 | 2.00±0.03 |
| 13.0 | 5.62±0.10 | | |

(A2)

$e^+$-$CO_2$

| $E$(eV) | $Q(10^{-16}$ cm$^2)$ | $E$(eV) | $Q(10^{-16}$ cm$^2)$ |
|---|---|---|---|
| 0.5 | 12.8 ±1.5 | 10.5 | 7.05±0.15 |
| 0.75 | 11.8 ±1.0 | 11.0 | 7.1 ±0.15 |
| 1.00 | 11.2 ±1.1 | 11.5 | 7.1 ±0.2 |
| 1.25 | 9.2 ±0.8 | 12.0 | 7.5 ±0.15 |
| 1.5 | 8.4 ±0.7 | 13.0 | 7.8 ±0.2 |
| 2.0 | 8.0 ±0.2 | 14.0 | 8.0 ±0.15 |
| 3.0 | 6.7 ±0.15 | 14.5 | 8.3 ±0.2 |
| 3.5 | 6.3 ±0.15 | 15.0 | 8.3 ±0.15 |
| 3.75 | 6.2 ±0.15 | 15.5 | 8.1 ±0.3 |
| 4.0 | 6.3 ±0.15 | 16 | 8.8 ±0.2 |
| 4.25 | 6.2 ±0.15 | 16.5 | 9.3 ±0.2 |
| 4.5 | 6.3 ±0.15 | 17 | 8.9 ±0.2 |
| 5.0 | 6.0 ±0.1 | 18 | 9.0 ±0.15 |
| 5.5 | 6.1 ±0.1 | 18.5 | 9.3 ±0.3 |
| 6.0 | 6.1 ±0.1 | 19 | 9.15±0.2 |
| 6.25 | 6.1 ±0.15 | 20 | 9.6 ±0.2 |
| 6.5 | 6.0 ±0.1 | 21 | 9.4 ±0.15 |
| 6.75 | 6.3 ±0.15 | 22 | 9.7 ±0.2 |
| 6.85 | 6.55±0.15 | 23 | 9.6 ±0.2 |
| 7.0 | 6.65±0.15 | 25 | 9.7 ±0.2 |
| 7.1 | 6.7 ±0.1 | 30 | 10.2 ±0.2 |
| 7.25 | 6.55±0.2 | 35 | 10.0 ±0.2 |
| 7.5 | 6.85±0.15 | 40 | 9.8 ±0.3 |
| 8.0 | 7.05±0.15 | 45 | 10.0 ±0.2 |
| 8.5 | 7.0 ±0.15 | 50 | 9.7 ±0.2 |
| 9.0 | 6.75±0.15 | 55 | 9.7 ±0.3 |
| 9.5 | 7.0 ±0.15 | 60 | 9.7 ±0.2 |
| 10.0 | 7.1 ±0.15 | | |

(A3)

$e^-$-$H_2$

| $E$(eV) | $Q(10^{-16}$ cm$^2)$ | $E$(eV) | $Q(10^{-16}$ cm$^2)$ |
|---|---|---|---|
| 2.0 | 17.0 ±0.1 | 35 | 4.66±0.03 |
| 2.9 | 17.3 ±0.2 | 40 | 4.30±0.01 |
| 3.9 | 17.6 ±0.13 | 45 | 3.98±0.01 |
| 4.9 | 15.6 ±0.07 | 50 | 3.66±0.09 |
| 6.8 | 14.3 ±0.07 | 75 | 2.92±0.02 |
| 8.8 | 12.2 ±0.09 | 100 | 2.56±0.04 |
| 10.8 | 10.56±0.04 | 150 | 1.98±0.01 |
| 12.9 | 9.48±0.03 | 200 | 1.69±0.03 |
| 14.9 | 8.48±0.02 | 300 | 1.27±0.03 |
| 20 | 6.72±0.04 | 400 | 1.04±0.03 |
| 25 | 5.79±0.04 | 500 | 0.87±0.02 |
| 30 | 4.92±0.05 | | |

(A4)

$e^-$-$N_2$

| $E$(eV) | $Q(10^{-16}$ cm$^2)$ | $E$(eV) | $Q(10^{-16}$ cm$^2)$ |
|---|---|---|---|
| 2.2 | 30.9±0.3 | 20 | 13.8 ±0.15 |
| 2.8 | 24.7±0.5 | 30 | 12.8 ±0.1 |
| 3.8 | 14.5±0.1 | 40 | 12.0 ±0.1 |
| 4.6 | 12.2±0.15 | 50 | 11.3 ±0.1 |
| 5.7 | 12.1±0.15 | 75 | 9.9 ±0.2 |
| 6.6 | 11.7±0.1 | 100 | 8.64±0.05 |
| 7.7 | 11.6±0.1 | 150 | 7.26±0.04 |
| 8.8 | 12.0±0.1 | 200 | 6.22±0.04 |
| 9.7 | 12.3±0.1 | 300 | 4.86±0.15 |
| 10.0 | 12.3±0.1 | 400 | 4.07±0.05 |
| 11.7 | 12.1±0.1 | 500 | 3.46±0.06 |
| 12.2 | 12.1±0.1 | 600 | 3.10±0.06 |
| 14.7 | 13.2±0.1 | 700 | 2.83±0.05 |

(A5)

$e^-$-$CO_2$

| $E$(eV) | $Q(10^{-16}$ cm$^2)$ | $E$(eV) | $Q(10^{-16}$ cm$^2)$ |
|---|---|---|---|
| 2.0 | 6.02±0.08 | 8.8 | 11.18±0.04 |
| 2.5 | 6.45±0.04 | 9.8 | 11.41±0.05 |
| 3.0 | 8.03±0.20 | 10.8 | 13.48±0.08 |
| 3.4 | 12.96±0.16 | 12.4 | 15.2 ±0.10 |
| 3.7 | 14.57±0.04 | 14.9 | 16.6 ±0.10 |
| 3.85 | 17.8 ±0.10 | 20 | 17.4 ±0.10 |
| 3.95 | 16.9 ±0.14 | 25 | 18.4 ±0.2 |
| 4.15 | 14.9 ±0.12 | 30 | 19.0 ±0.2 |
| 4.4 | 13.56±0.08 | 35 | 18.0 ±0.3 |
| 4.9 | 10.12±0.20 | 40 | 17.7 ±0.1 |
| 5.9 | 8.70±0.25 | 45 | 17.0 ±0.1 |
| 6.4 | 8.73±0.04 | 50 | 15.7 ±0.1 |
| 7.3 | 9.97±0.07 | | |

(A6)

*Present address: Energy Conversion Devices Inc., Troy, Michigan 48084.
†Present address: Department of Physics, Yarmouk University, Irbid, Jordan.
‡Present address: Bell Laboratories, Allentown, Pennsylvania 18103.
§Present address: Johns Hopkins University, Applied Physics Laboratory, Laurel, Maryland 20810.

[1]E. L. Chupp, D. J. Forrest, P. R. Higbie, A. N. Suri, C. Tsai, and P. P. Dunphy, Nature (London) 241, 333 (1973).
[2]M. Leventhal, C. J. MacCallum, and P. D. Stang, Astrophys. J. 225, L11 (1978).
[3]C. J. Crannell, G. Joyce, R. Ramaty, and C. Werntz, Astrophys. J. 210, 582 (1976).
[4]R. W. Bussard, R. Ramaty, and R. J. Drachman, Astrophys. J. 228, 928 (1979).
[5]H. S. W. Massey, Phys. Today 29, No. 3, 42 (1976).
[6]D. E. Golden, N. F. Lane, A. Temkin, and E. Gerjuoy, Rev. Mod. Phys. 43, 642 (1971).
[7]N. F. Lane, Rev. Mod. Phys. 52, 29 (1980).
[8]G. J. Schulz, Rev. Mod. Phys. 45, 423 (1973).
[9]T. C. Griffith and G. R. Heyland, Phys. Rep. 39, 169 (1978); T. C. Griffith, Adv. At. Mol. Phys. 15, 135 (1979).
[10]W. E. Kauppila, T. S. Stein, J. H. Smart, and V. Pol., in *Abstracts of the Tenth ICPEAC, Paris, 1977,* edited by M. Barat and J. Reinhardt (Commissariat a L'Energie Atomique, Paris, 1977), p. 826.
[11]W. E. Kauppila, T. S. Stein, and G. Jesion, Phys. Rev. Lett. 36, 580 (1976).
[12]W. E. Kauppila, T. S. Stein, G. Jesion, M. S. Dababneh, and V. Pol, Rev. Sci. Instrum. 48, 822 (1977).
[13]T. S. Stein, W. E. Kauppila, V. Pol, J. H. Smart, and G. Jesion, Phys. Rev. A 17, 1600 (1978).
[14]M. S. Dababneh, W. E. Kauppila, J. P. Downing, F. Laperriere, V. Pol, J. H. Smart, and T. S. Stein, Phys. Rev. A 22, 1872 (1980).
[15]W. E. Kauppila, T. S. Stein, J. H. Smart, M. S. Dababneh, Y. K. Ho, J. P. Downing, and V. Pol, Phys. Rev. A 24, 725 (1981).
[16]T. S. Stein, W. E. Kauppila, and L. O. Roellig, Phys. Lett. 51A, 327 (1975).
[17]P. G. Coleman, T. C. Griffith, G. R. Heyland, and T. R. Twomey, private communication, as reported by Griffith and Heyland in Phys. Rep. (Ref. 9).
[18]M. Charlton, T. C. Griffith, G. R. Heyland, and G. L. Wright, J. Phys. B 13, L353 (1980).
[19]P. Baille, J. W. Darewych, and J. G. Lodge, Can. J. Phys. 52, 667 (1974).
[20]S. Hara, J. Phys. B 7, 1748 (1974).
[21]P. G. Coleman, T. C. Griffith, and G. R. Heyland, Appl. Phys. 4, 89 (1974).
[22]M. Charlton, T. C. Griffith, G. R. Heyland, K. S. Lines, and G. L. Wright, J. Phys. B 13, L757 (1980).
[23]E. Bruche, Ann. Phys. (Leipzig) 82, 912 (1927).
[24]C. Ramsauer and R. Kollath, Ann. Phys. (Leipzig) 4, 91 (1930).
[25]D. E. Golden, H. W. Bandel, and J. A. Salerno, Phys. Rev. 146, 40 (1966).
[26]J. Ferch, W. Raith, and K. Schroder, J. Phys. B 13, 1481 (1980).
[27]B. van Wingerden, R. W. Wagenaar, and F. J. de Heer, J. Phys. B 13, 3481 (1980).
[28]G. Dalba, P. Fornasini, I. Lazzizzera, G. Ranieri, and A. Zecca, J. Phys. B 13, 2839 (1980).
[29]R. L. Wilkins and H. S. Taylor, J. Chem. Phys. 47, 3532 (1967).
[30]S. Hara, J. Phys. Soc. Jpn. 27, 1009 (1969).
[31]R. J. W. Henry and N. F. Lane, Phys. Rev. 183, 221 (1969).
[32]P. G. Coleman, T. C. Griffith, G. R. Heyland, and T. L. Killeen, *Atomic Physics* 4, (Plenum, New York, 1975), p. 355.
[33]J. W. Darewych and P. Baille, J. Phys. B 7, L1 (1974).
[34]E. S. Gillespie and D. G. Thompson, J. Phys. B 8, 2858 (1975).
[35]D. E. Golden, Phys. Rev. Lett. 17, 847 (1966).
[36]R. E. Kennerly, Phys. Rev. A 21, 1876 (1980).
[37]H. J. Blaauw, R. W. Wagenaar, D. H. Barends, and F. J. de Heer, J. Phys. B 13, 359 (1980).
[38]G. Dalba, P. Fornasini, R. Grisenti, G. Ranieri, and A. Zecca, J. Phys. B 13, 4695 (1980).
[39]N. Chandra and A. Temkin, Phys. Rev. A 13, 188 (1976).
[40]N. Chandra and A. Temkin, J. Chem. Phys. 65, 4537 (1976).
[41]E. Bruche, Ann. Phys. (Leipzig) 83, 1065 (1927).
[42]C. Ramsauer, Ann. Phys. (Leipzig) 83, 1129 (1927).
[43]C. Szmytkowski and M. Zubek, Chem. Phys. Lett. 57, 105 (1978).
[44]J. Ferch, C. Masche, and W. Raith, J. Phys. B 14, L97 (1981).
[45]M. A. Morrison, N. F. Lane, and L. A. Collins, Phys. Rev. A 15, 2186 (1977).